Author: Ren, Haoran; Lin, Han; Li, Xiangping; Gu, Min
Title: Three-dimensional parallel recording with a Debye diffraction-limited and aberration-free volumetric multifocal array
Year: 2014
Journal: Optics Letters
Volume: 39
Issue: 6
Pages: 1621-1624
URL: ttp://hdl.handle.net/1959.3/376778

Three-dimensional parallel recording with a Debye diffraction-limited and aberration-free volumetric multifocal array

Haoran Ren, Han Lin, Xiangping Li and Min Gu

Centre for Micro-Photonics, Faculty of Engineering and Industrial Sciences, Swinburne University of Technology, P.O. Box 218, Hawthorn, Victoria 3122, Australia

*Corresponding author: mgu@swin.edu.au

Abstract

In this paper, we report on the generation of high-quality Debye diffraction-limited volumetric multifocal arrays. The multifocal arrays with a uniformity of 0.99 over the entire focal region of a high numerical-aperture objective are volumetrically generated by using the vectorial Debye-based three-dimensional Fourier transform method through the accurate phase modulation on an Ewald cap. Thus, this method is capable of dynamic spherical aberration compensation. Applying this feature into three-dimensional parallel aberration-free optical recording reveals a significant increase in the throughput by two orders of magnitude.

The ever-increasing demand for high storage capacity has compelled the technique revolution of three-dimensional (3D) optical data storage where information can be stored in the volume of a disc [1]. Even though an ultra-high storage density can be achieved by focusing a pulsed laser beam with a high numerical aperture (NA) objective [2], the associated bit-sequential recording is intrinsically slow, representing a fundamental bottleneck for ultra-high throughputs, which are equally important for the next generation ultra-high capacity 3D optical storage devices.

On the other hand, computer-addressed spatial light modulators (SLMs) with phase-only modulation have opened the perspective to generate multifocal arrays for fast and parallel laser processing [3]. As such, the vectorial Debye-based two-dimensional Fourier transform (2D-FT) method for considering the depolarization effect by a high NA objective, which is a necessity for ultra-high capacity volumetric optical storage, has facilitated the generation of diffraction-limited planar multifocal arrays through the accurate phase modulation [4,5]. Even though superposing phase patterns of light fields from multiple discrete focal planes [6-9] provides the possibility to create volumetric multifocal arrays without considering the light fields within the entire focal region, the 2D-FT method accompanied with interlayer cross talks fails to generate diffraction-limited volumetric multifocal arrays with a high uniformity. However, a diffraction-limited volumetric multifocal array based on a high NA objective is essential for ultra-high throughput in 3D optical storage, but has never been achieved yet.

In this paper, we report on the generation of diffraction-limited volumetric multifocal arrays using the vectorial Debye-based 3D-FT method. Unlike the 2D-FT method [4,5], the proposed vectorial Debye-based 3D-FT method generates the accurate phase modulation on an Ewald cap by numerically considering the multilayered light fields and thus allows for diffraction-limited volumetric multifocal arrays with diminished cross talks and hence a high uniformity. By implementing the accurate phase modulation into the laser beam through an SLM, diffraction-limited volumetric multifocal arrays with arbitrary intensity configurations can be simultaneously recorded in the volume of the recording media in a single laser shot. Moreover, the proposed method allows for the integration with aberration compensation methods for 3D parallel aberration-free recording with an increased throughput by two orders of magnitude.

The experimental configuration and the principle of the accurate phase retrieval process are depicted in Fig. 1. The key physical step is to obtain the phase distribution on the Ewald cap by the inverse 3D-FT [11-14] of the entity fields and to calculate the volumetric intensity distribution in the focal region by using the vectorial Debye theory [15, 16]. A 3D entity field can be written as $\sum_{i=1}^{M} I_i^d \delta(x_i, y_i, z_i)$, where M denotes the total foci number and I_i^d denotes the desired peak intensity of ith focal spot. Meanwhile, a 3D weighting factor w defined as $w^n = w^{n-1} \frac{\sum_{i=1}^{M} abs(E(x_i, y_i, z_i))}{M * abs(E(x_i, y_i, z_i))}$ ($w^0 = 1$) is embedded to individually manipulate the intensity distribution in a volumetric multifocal array, where n is the iteration number. Finally, the 2D phase modulation at the back aperture of the high NA objective can be obtained by a parallel projection from the 3D Ewald cap, as shown in Fig. 1.

Instead of superposing phase patterns of light fields from multiple discrete focal planes separated by corresponding lens phase factors [6-9], the vectorial Debye-based 3D-FT method allows for considering the entire focal region as an entity. As such, the interlayer cross talks can be minimized. To quantity this, a uniformity factor is defined as $u = 1 - \frac{I_{\max} - I_{\min}}{I_{\max} + I_{\max}}$ [17], where $I_{\max}$ and $I_{\min}$ are the maximum and minimum intensities in foci. Figure 2 shows the comparison between the vectorial Debye-based 3D-FT and 2D-FT methods with NA=1.4 and wavelength of 800 nm for an x-linearly polarized light. The 3D-FT method is superior to the 2D-FT method as the complexity of the volumetric multifocal arrays is increased. Fig. 2(a) shows that the uniformity of the 2D-FT method tends to drop obviously as the foci number in each plane is increased up to 10, however, the uniformity of the 3D-FT method remains unaffected with a value of 0.99. More importantly, Fig. 2(b) demonstrates that the 3D-FT approach performs better with different axially separated distances, owing to the fact that it considers the volumetric multifocal arrays as an entity field rather than multiple discrete focal planes. When the axial distance between multilayered focal arrays reduces, the interlayer cross talks appear more significantly and degrade the uniformity by the conventional 2D-FT methods. The 3D-FT method can eliminate the cross talks from intermediate planes. As a result, a high uniformity can be remained. As an example, the superior performance of 3D-FT can be clearly seen in the simulated results with an interlayer distance of 3 μm as shown in Figs. 2(c) and 2(d).

Applying the proposed method for fast parallel optical recording in two-photon (2P) induced multilayer optical data storage in a photoreduction polymer can lead to two orders of magnitude increase in throughput. To this purpose, we used a linearly polarized femtosecond pulsed beam at the wavelength of 800 nm from an amplified Ti-sapphire system (Spitfire, Newport/Spectra Physics, 100 fs pulse duration, 1kHz repetition rate) to illuminate a refractive SLM (Holoeye Pluto, 1080× 1920 pixels, 256 gray levels). The phase modulation displayed on the SLM was relayed to the back aperture of a high NA objective (Olympus, 100×, UPLSAPO, 1.40 NA) through a 4f telescope composed of lens L1 (500 mm) and L2 (300 mm). A photoreduction polymer (refractive index of 1.50 at 800 nm) consisting of 16 mg of $HAuCl_4$, 0.67 mg of R6G, and 570 mg of Poly (methyl methacrylate) (PMMA) was prepared as the recording sample [18]. An enhanced fluorescence emission from R6G dye molecules in the focal spot can be employed as the mechanism for recording and readout [18]. A volumetric multifocal array consisting of three layered patterns of "1", 2" and "3" in focal region with z=-3 μm, z=0 and z=3 μm were recorded in a single slight deviation might be attributed to the spatially inhomogeneous response of the recording sample. The demonstrated method can potentially increase the throughput of 3D optical storage by two-order of magnitude compared with the traditional bit-sequential approach.

The vectorial Debye-based 3D-FT method offers not only the accurate phase for volumetric multifocal arrays with a high uniformity but also the capability of dynamic aberration compensation in the recording medium. Spherical aberration (SA) caused by the refractive-index mismatch which can significantly degrade the recording performance [8, 19-

22], can now be dynamically compensated for the entire focal region. To this purpose, a volumetric compensation factor $\sum_{i=1}^{M} I_i^d \delta(x_i, y_i, z_i) \cdot \exp[-i\Phi_{SA}(z_i)]$ is added, where $\Phi_{SA}(z_i) = kz_i(n_2 \cos\theta_2 - n_1 \cos\theta_1)$ denotes the SA term of the focal position ($z = z_i$) by assuming that the origin of the coordinates is at the interface between the immersion oil and the sample, k denotes the wave-number, θ_1 and θ_2 are the converging angles in the immersion and recording media of refractive indices of n_1 and n_2, respectively. To experimentally confirm the SA compensation capability, a photochromic polymer sample (refractive index of 1.69 at 800 nm) with dark focal spots due to the fluorescence emission reduction was prepared [23]. Three layered patterns located at $z = 1\mu m, z = 6\mu m, z = 11\mu m$ with and without the SA compensation were recorded and retrieved, respectively, as shown in Figs.4. In the absence of the SA compensation, only the first layer ($z = 1\mu m$) information which suffers negligible SA can be retrieved, while patterns in the other two layers were severely degraded and cannot be retrieved, as shown in Fig. 4(a). On the other hand, the volumetric layered information can be clearly retrieved provided the SA can be compensated in the 3D-FT methods as shown in Fig. 4(c). The axial point spread functions (PSFs) of the recorded foci in three layers were obtained by scanning the fluorescence intensity along the axial direction. It is clearly seen that significant aberration is present before the SA compensation, and the recorded bits suffer from peak intensity drop, axial elongation and focusing shift, as shown in Fig. 4(b). In contrast, the disruptive aberration effects observed above can be removed through integrating the SA compensation, as shown in Fig. 4(d).

In conclusion, we have developed an accurate phase modulation method for the diffraction-limited volumetric multifocal arrays under high NA objectives. The proposed vectorial Debye-based 3D-FT methods allow for the generation of volumetric multifocal arrays with diminished interlayer cross talks and aberration free with integrated aberration compensation approaches. In principle, the maximal lateral and axial sizes of a volumetric multifocal array are determined by the field of view and the working distance of a high NA objective using the vectorial Debye-based 3D-FT method. The computation speed of the proposed method is also very fast. For a comparison, a volumetric multifocal array consisted of a stack of discrete layers, the computation time are almost identical to the conventional 2D-FT method. Even for a planar multifocal array, 3D-FT method takes only seven times longer than the 2D-FT method. The demonstrated diffraction-limited and aberration-free volumetric multifocal arrays may open the new perspective for wide applications in ultra-high density optical storage [24, 25], parallel imaging microscopy [5], direct laser writing [26, 27] and optical tweezers [28].

Acknowledgement

This work is supported by the Australian Research Council (ARC) Laureate Fellowship scheme (FL100100099).

References

[1]. Dimitri A. Parthenopoulos and Peter M. Rentzepis, "Three-dimensional optical storage memory," Science **245**, 843-845 (1989).

[2]. Peter Zijlstra, James W. M. Chon and Min Gu, "Five-dimensional optical recording mediated by surface plasmons in gold nanorods," Nature **459**, 410-413 (2009).

[3]. David G. Grier, "A revolution in optical manipulation," Nature **424**, 810-816 (2003).

[4]. Han Lin, Baohua Jia and Min Gu, "Dynamic generation of Debye diffraction-limited multifocal arrays for direct laser printing nanofabrication." Optics Letters. **36**(3), 406-408 (2011).

[5]. Min Gu, Han Lin and Xiangping Li, "Parallel multiphoton microscopy with cylindrically polarized multifocal arrays," Optics Letters. **38**(18), 3627-3630 (2013).

[6]. T. Haist, M. Schonleber and H. J. Tiziani, "Computer-generated holograms from 3D-objects written on twisted-nematic liquid crystal displays," Optics Communication. **140**, 299-308 (1997).

[7]. Roberto Di Leonardo, Francesca Ianni and Giancarlo Ruocco, “Computer generation of optimal holograms for optical trap arrays,” Optics Express. **15**(4), 1913-1922 (2007).

[8]. Alexander Jesacher and Martin J. Booth, “Parallel direct laser writing in three dimensions with spatially dependent aberration correction,” Optics Express. **18**(20), 21090-21099 (2010).

[9]. Erik H. Waller and Georgvon Freymann, “Multi foci with diffraction limited resolution,” Optics Express. **21**(18), 21708-21713 (2013).

[10]. R. W. Gerchberg and W. O. Saxton, “A practical algorithm for the determination of phase from image and diffraction image and diffraction plane pictures,” Optik. **35**, 237-246 (1972).

[11]. C. W. McCutchen, “Convolution relation within the three-dimensional diffraction image,” Journal of the Optical Society of America. A. **8**(6), 868–870 (1991).

[12]. GalShabtay, “Three-dimensional beam forming and Ewald’s surfaces,” Optics Communications. **226**(1-6), 33-37(2003).

[13]. J. Lin, O. G. Rodriguez-Herrera, F. Kenny, D. Lara and J. C. Dainty, "Fast vectorial calculation of the volumetric focused field distribution by using a three-dimensional Fourier transform," Optics Express. **20**(2), 1060-1069 (2012).

[14]. Graeme Whyte and Johannes Courtial, "Experimental demonstration of holographic three-dimensional light shaping using a Gerchberg-Saxton algorithm," New Journal of Physics. **7**(117), 2-11 (2005).

[15]. Min Gu, Advanced Optical Imaging Theory (Springer Verlag, Heidelberg, 2000).

[16]. E. Wolf, "Electromagnetic diffraction in optical systems, I. An integral representation of the image field," Proceedings of the Royal Society. London. A **253**, 349-357 (1959).

[17]. Marco Polin, Kosta Ladavac, Sang-Hyuk Lee, Yale Roichman and David G. Grier, "Optimized holographic optical traps," Optics Express. **13**(15), 5831-5845 (2005).

[18]. Xiangping Li, Yaoyu Cao and Min Gu, "Superresolution-focal-volume induced 3.0 Tbytes/ disk capacity by focusing a radially polarized beam," Optics Letters. **36**(13), 2510-2512 (2011).

[19]. P. Torok, P. Varga, Z. Laczik, G. R. Booker, "Electromagnetic diffraction of light focused through a planar interface between materials of mismatched refractive

indices: structure of the electromagnetic field. I" Journal of the Optical Society of America. A. **12**(10), 2136-2144 (1995).

[20]. Daniel Day and Min Gu, "Effects of refractive-index mismatch on three-dimensional optical data –storage density in a two-photon bleaching polymer" Applied Optics. **37**(26), 6299-6304 (1998).

[21]. Benjamin P. Cumming, Alexander Jesacher, Martin J. Booth, Tony Wilson and Min Gu, "Adaptive aberration compensation for three-dimensional micro-fabrication of photonic crystals in lithium niobate" Optics Express. **19**(10), 9419-9425 (2011).

[22]. Benjamin P. Cumming, Sukanta Debbarma, Barry Luther-Davies and Min Gu, "Effect of refractive index mismatch aberration in arsenic trisulfide" Applied Physics. B. **109**(2), 227-232 (2012).

[23]. Xiangping Li, James W.M. Chon, Richard. A. Evans and Min Gu, "Two-photon energy transfer enhanced three-dimensional optical memory in quantum-dot and azo-dye doped polymers," Applied Physics Letters. **92**, 063309 (2008).

[24]. Min Gu and Xiangping Li, "The road to multi-dimensional bit-by-bit optical data storage," Optics and Photonics News. **21** (7), 29-33 (2010).

[25]. Xiangping Li, Tzu-Hsiang Lan, Chung-HaoTien and Min Gu, "Three-dimensional orientation-unlimited polarization encryption by a single optically configured vectorial beam," Nature Communication. **3**, 998 (2012).

[26]. Zongsong Gan, Yaoyu Cao, Richard A. Evans and Min Gu, "Three-dimensional deep sub-diffraction optical beam lithography with 9nm feature size," Nature Communication. **4**, 2061 (2013).

[27]. Kai Lou, Shengxia Qian, Zhicheng Ren, Chenghou Tu, Yongnan Li and Huitian Wang, "Femtosecond laser processing by using patterned vector optical fields," Scientific Report. **3**, 2281 (2013).

[28]. Mathieu L Juan, Maurizio Righini and Romain Quidant, "Plasmon nano-optical tweezers," Nature Photonics. **5**, 349-356 (2011).

Figure 1. Schematic diagram of generating a volumetric multifocal array through an SLM. Vectorial Debye-based 3D-FT imposing on the 3D Ewald cap located in the aperture space provides a volumetric intensity distribution in the focal region. Phase pattern displayed on the SLM can be obtained by a parallel projection of the 3D Ewald cap. L1, L2 are telescope lenses.

Figure 2. Comparison of the uniformity of volumetric multifocal arrays derived from the vectorial Debye-based 3D-FT and 2D-FT methods. Volumetric multifocal arrays are arranged in three focal planes. (a) Comparison with different foci number in each plane (axial separation is set to $5\,\mu m$). (b) Comparison with different axial separated distances (total foci number is kept at 108). An example of intensity distribution of three foci within the xz-plane achieved by (c) the 2D-FT method and (d) the 3D-FT method.

Figure 3. Simulated (a)-(c) and experimental (d)-(f) results of a volumetric multifocal array in a recording media. (g) and (h) Enlarged single foci images labeled as “1” and “2” in (b) and (e). (i)-(j) The intensity plot along the x and the y directions of (g) and (h), respectively.

Figure 4. Experimental results of a volumetric multifocal array recorded in three focal planes of (a) before and (c) after the SA compensation. Axial PSFs of three recorded foci in three layers (b) without and (d) with the SA compensation are obtained from the fluorescence intensity variations.

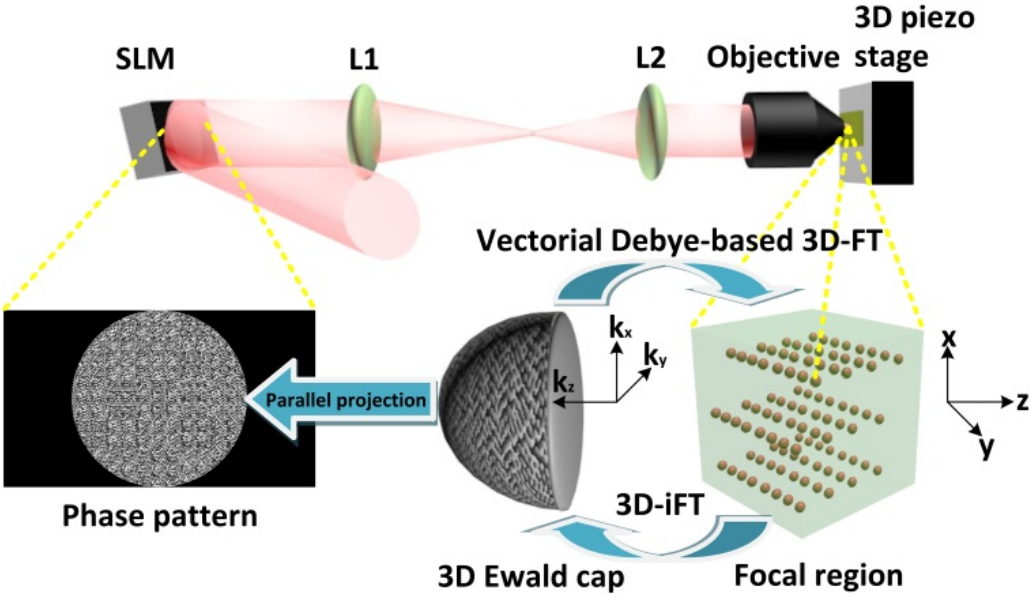

3D piezo stage
SLM
L1
L2
Objective
Vectorial Debye-based 3D-FT
Parallel projection
Phase pattern
3D-iFT
3D Ewald cap
Focal region

Figure 1

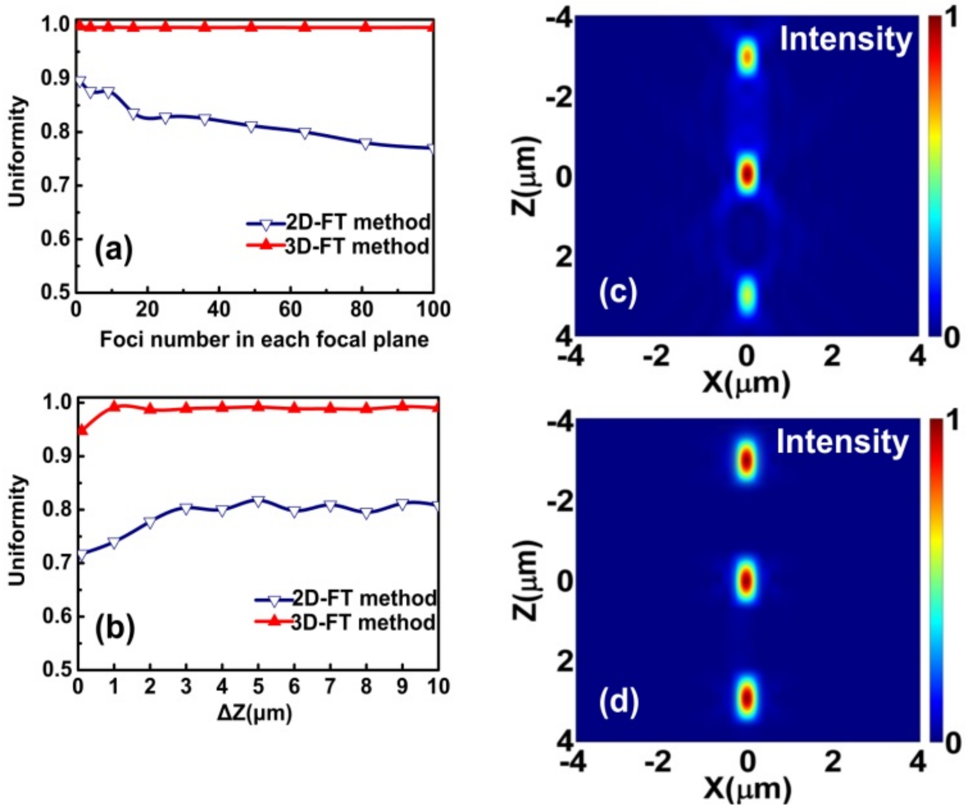

(a)
Uniformity
Foci number in each focal plane
2D-FT method
3D-FT method
(b)
Uniformity
ΔZ(μm)
2D-FT method
3D-FT method
(c)
Intensity
Z(μm)
X(μm)
(d)
Intensity
Z(μm)
X(μm)

Figure 2

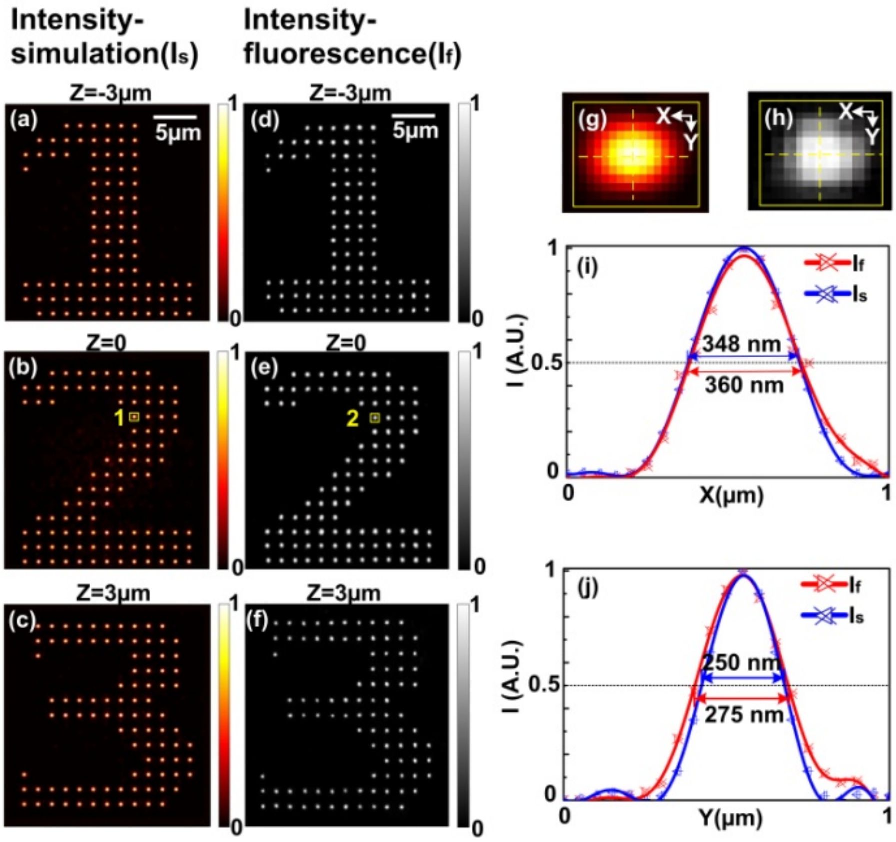

Intensity-simulation(Is)
Intensity-fluorescence(If)
Z=-3μm
Z=0
Z=3μm
(a)
(b)
(c)
(d)
(e)
(f)
(g)
(h)
(i)
(j)
5μm
1
2
348 nm
360 nm
250 nm
275 nm
I (A.U.)
X(μm)
Y(μm)
If
Is

Figure 3

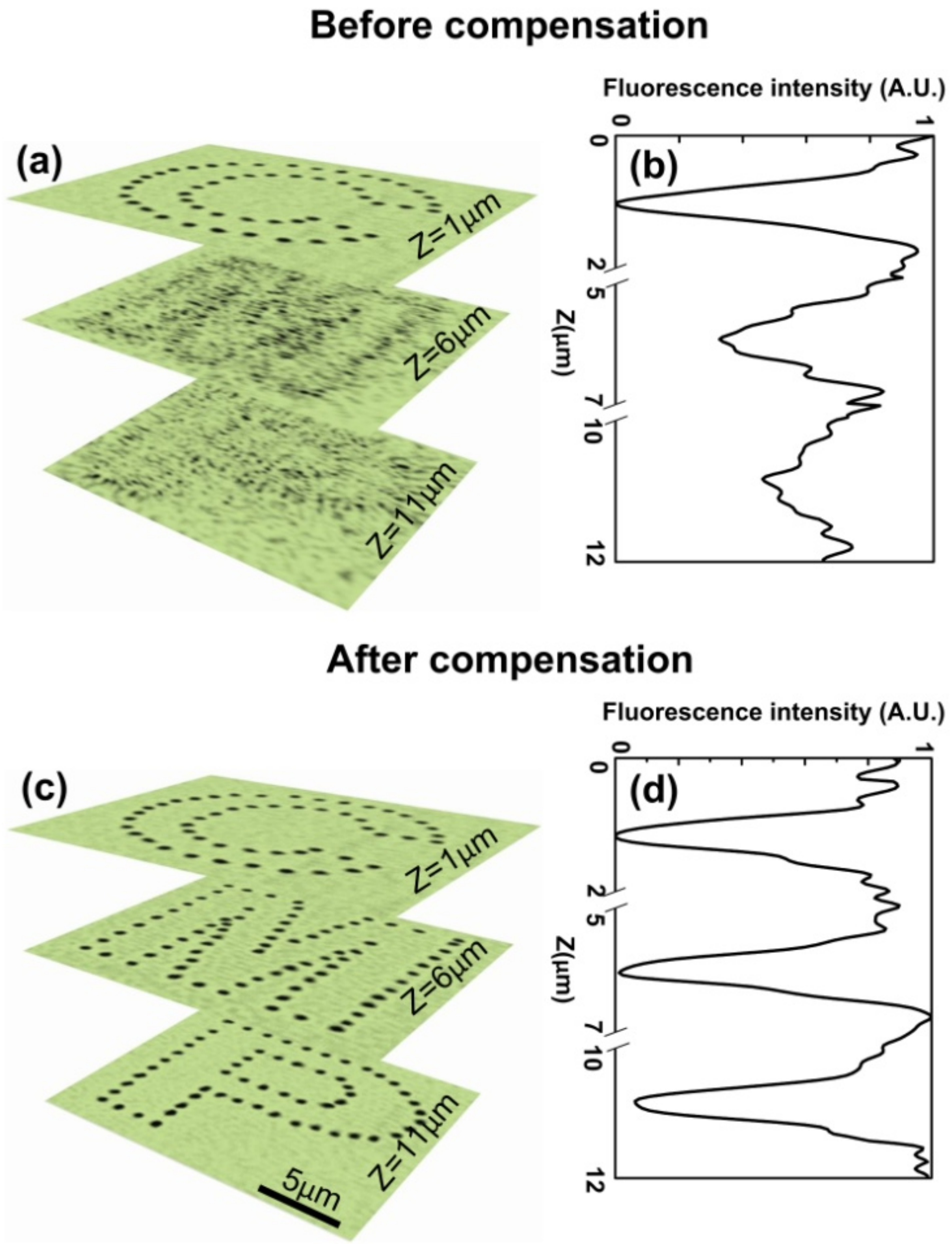
Before compensation
Fluorescence intensity (A.U.)
(a)
(b)
Z=1μm
Z=6μm
Z=11μm
Z(μm)
0
1
2
5
7
10
12
After compensation
Fluorescence intensity (A.U.)
(c)
(d)
5μm

Figure 4